Temperature dependence of the nonlinear optical response of smectic liquid crystals containing gold nanorods

R. S. Silva,[1] P. B. de Melo,[1] L. Omena,[1] A. M. Nunes,[2] M. G. A. da Silva,[2] M. R. Meneghetti,[2] and I. N. de Oliveira[1]
[1]*Instituto de Física, Universidade Federal de Alagoas, 57072-970 Maceió, Alagoas, Brazil*
[2]*Instituto de Química e Biotecnologia, Universidade Federal de Alagoas, 57072-970 Maceió, Alagoas, Brazil*
(Received 27 June 2017; published 18 December 2017)

The present study is devoted to the investigation of the nonlinear optical properties of a smectic liquid crystal doped with gold nanorods. Using the Z-scan technique, we investigate the changes in the optical birefringence of a homeotropic sample upon laser exposure, considering the configurations of normal and oblique incidence. Our results reveal that the birefringence variations may be governed by distinct physical mechanisms, depending on the relative angle between the far-field director and the wave vector of the excitation laser beam. In particular, we observe that the position dependence of the far-field transmittance exhibits different behaviors as the incidence angle is changed, indicating that distortions in the beam wavefront may be associated with the thermal lens phenomenon or an optically induced reorientation of the nematic director. The temperature dependence of the nonlinear refractive and absorptive coefficients is investigated close to the smectic-A–nematic phase transition. A detailed analysis of the interplay between smectic order and plasmon resonance is performed, thus unveiling the capability of plasmonic liquid crystal to be used in optical devices.

DOI: 10.1103/PhysRevE.96.062703

I. INTRODUCTION

Colloidal liquid crystals constitute an important class of soft materials, where the interplay between the guest-host interaction and the emergence of elastic distortions gives rise to a large variety of fascinating phenomena. In this context, liquid crystals doped with metallic nanoparticles have attracted a remarkable amount of interest over the past decade, due to the possibility of using them as the active materials in electro-optical devices with tunable optical properties [1–5]. In particular, the reorientation of the nematic director has been successfully used as an efficient mechanism to tune the plasmon resonance of guest nanoparticles [3,6–8]. Therefore, plasmonic liquid crystals have emerged as a promising system for the development of plasmonic color filters [3,7], tunable metamaterials [9,10], and sensors [11,12]. Further, the addition of gold nanoparticles has been identified as a feasible alternative to improve different physical properties of liquid-crystalline systems, such as the optical and electric Fréedericksz thresholds [13], birefringence [14], and elastic constants [15].

Several studies have investigated the contribution of the surface plasmon resonance to the linear and nonlinear optical properties of liquid crystals doped with gold nanoparticles [6,9,13,14,16–18]. In particular, the plasmon excitation affects the real and imaginary parts of the refractive indices of the liquid-crystal hosts [6,9,14], due to the emergence of a local electric field and the subsequent modification of the orientational ordering around the guest nanoparticles. In fact, a reversible orientational switch from the homeotropic to the planar configuration has been obtained in nematic films from the amplification of the localized electric field generated by the optical excitation of gold nanorods [9]. Moreover, it has been observed that the addition of gold nanoparticles induces a significant increase in the diffraction efficiency of nematic samples, which is mainly associated with a thermal variation in the sample birefringence [17,19–21]. Actually, guest nanoparticles behave as heat sources upon reasonable laser exposure, thus leading to an enhancement in the thermal-optical coefficient of the samples [16,22]. Such a plasmonic photoheating effect has been exploited in the suppression of the typical reflection band of cholesteric liquid crystals [23].

Although the plasmonic effects on the thermal and optical properties of nematic liquid crystals have been widely analyzed, only a few studies have been devoted to the investigation of smectic samples doped with gold nanoparticles [9,24–27]. However, colloidal smectic systems exhibit a rich phenomenology associated with the quasi-long-range positional order that characterizes the stratified structure of smectic phases. A prominent example is the formation of stable dispersions of gold nanospheres in smectic-A films supported on solid substrates [9], where a progressive redshift is observed in the absorption spectra as the concentration of nanoparticles is increased. In particular, atomic force microscopy images of such films revealed that the layered structure of the smectic phase prevents the irreversible aggregation of gold nanoparticles exhibiting a diameter larger than the layer spacing [9,24]. Close to the nematic–smectic-A phase transition, thermal lens measurements in homeotropic samples showed that the critical behaviors of the thermo-optical coefficient and the thermal diffusivity are sensitive to the shape of gold nanoparticles [26]. Further, a nonlinear absorptive phenomenon was observed in smectic samples containing gold nanorods [26], indicating that the emergence of smectic order affects the alignment of the particles. In fact, it has been observed that dislocations in the smectic ordering induce the self-assembly of nanoparticles immersed in samples under hybrid boundary conditions [28,29]. In ferroelectric smectic liquid crystals, the introduction of gold nanospheres leads to a pronounced increase in the optical tilt [27], which is accompanied by the reduction of the threshold voltage and the enhancement of optical contrast.

The present study is devoted to the characterization of the nonlinear optical properties of a smectic liquid crystal doped with gold nanorods. By using the Z-scan technique, we investigate the changes in the optical birefringence of a homeotropic sample upon the laser exposure. Our results

show that the position dependence of the far-field transmittance exhibits different behaviors as the incidence angle is changed, indicating that distortions in the beam wavefront are governed by different physical mechanisms. More specifically, we observe that a photoinduced reorientation takes place as the sample is excited in the oblique incidence geometry, being characterized by a nonlinear optical contribution to the liquid-crystal birefringence. Such a result contrasts with Z-scan measurements performed in the normal incidence geometry [26], where the changes in the liquid-crystal birefringence were associated with the heat generation by the gold nanorods during the laser exposure. Further, we investigate the temperature dependence of the nonlinear refractive and absorptive coefficients close to the smectic-A–nematic phase transition. Although the saturation of the nonlinear absorption has been previously reported [26], the present study reveals a gradual increase of the nonlinear absorption coefficient as the temperature is reduced well below the nematic–smectic-A transition temperature, reflecting the ordering degree of nanorods inside the smectic host. The emergence of an optical nonlinearity in smectic samples is analyzed, giving emphasis to the effects associated with the introduction of gold nanorods.

II. MATERIALS AND METHOD

Gold nanorods were prepared in aqueous solution by the seed-mediated method [30], with cetyltrimethylammonium bromide as the capping agent. Such a capping agent stays stable during the exchange of solvents and subsequent transfer process to the liquid crystal, with a homeotropic anchoring being expected at the colloid surface. We synthesized gold nanorods, presenting an average length $L = 40$ nm, with an aspect ratio around $r = 2.5$ (see the inset of Fig. 1). The analysis of the size and shape of gold nanorods was performed using a FEI-Tecnai 20 transmission electron microscope operating at 200 kV or a FEI-Morgani 268D operating at 100 kV, with the samples being prepared according to Ref. [30]. Micrographs

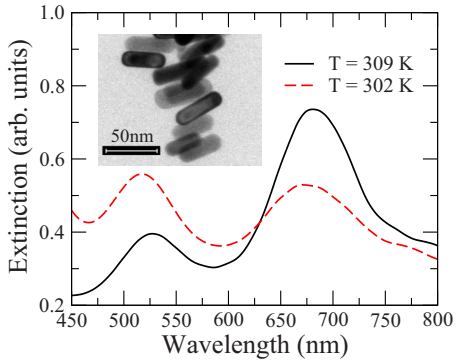

FIG. 1. Extinction spectra of a homeotropic 8CB sample containing gold nanorods at distinct temperatures: $T = 309$ K (black solid line), corresponding to the nematic phase, and $T = 302$ K (red dashed line), corresponding to the smectic-A phase. Notice that the transversal and longitudinal plasmon bands are highly sensitive to the sample temperature, indicating that the nematic and smectic ordering play an important role in the mean alignment of anisotropic guest particles. The inset shows a TEM image of the gold nanorods dispersed in the liquid crystal host.

from transmission electron microscopy (TEM) were evaluated using the Sigma Scan program to determine the particle size distribution, measuring approximately 100 nanoparticles in the sample. In order to obtain well-separated guest particles, the studied nanoparticles were dispersed in the compound 4-octyl-4′-cyanobiphenyl (8CB) at a low weight concentration ($c = 0.02$ wt. %), where no visible aggregates were observed in the resultant system. The 8CB exhibits an isotropic-nematic phase transition at $T_{NI} = 313.5$ K and a nematic–smectic-A transition at $T_{AN} = 306.5$ K. This compound exhibits a good chemical stability upon laser exposure and it was purchased from Sigma-Aldrich, being used without further purification. Homeotropic samples were prepared by treating cleaned glass surfaces with the octadecyltrichlorosilane surfactant (Sigma-Aldrich). Spacers were used to maintain the cell thickness at $\ell_0 = 100$ μm. The cells were filled by capillary action in the isotropic phase of 8CB ($T \approx 323$ K) and slowly cooled down to the room temperature. Samples were observed under a crossed-polarized microscope to ensure alignment and uniformity. Further, the extinction spectra of filled cells were recorded using a UV-visible spectrometer (USB2000, Ocean Optics). Samples were placed in a temperature-controlled oven within the accuracy of 0.1 K, with the sample temperature being varied in steps of $\Delta T = 0.2$ K, at a rate of 0.1 K/min. After reaching the target temperature, the measurements were performed after a waiting time of 20 min in order to certify that the system had reached the equilibrium configuration.

Aiming the investigation of the nonlinear optical properties of gold nanorods dispersion in smectic liquid crystals, we employed the Z-scan technique using a linearly polarized cw diode-pumped solid state laser at $\lambda = 532$ nm as the light source. The laser beam presented a Gaussian profile with a well-defined vertical polarization and the laser power used to excite the sample was $P = 1.0$–4.0 mW. The laser beam was focused by a lens with a focal length of 15 cm, which provided a minimum waist of $w_0 = 50$ μm, resulting in a confocal distance $z_c = 14.7$ mm. The sample was moved back and forth along the z axis around the minimum beam waist of the laser during the measurement, with a single displacement step of 5 mm. By using an iris centered along the beam propagation direction, the far-field transmittance was measured as a function of the sample position z in the configurations of closed ($S = 0.1$) and fully open ($S = 1$) iris apertures. All measurements were performed in duplicate, where identical results were obtained. The samples were excited in different incidence geometries, being determined by the relative angle between the unperturbed nematic director and propagation direction ϕ.

III. THE Z-SCAN BACKGROUND

A. Closed-aperture configuration

In a Z-scan measurement with a closed aperture, the far-field transmittance depends on the position of the sample, which behaves itself as a lenslike optical element that introduces a phase shift in the beam wavefront. In particular, self-focusing or defocusing behavior in the beam center is observed due to changes in the refractive index of the sample upon high-intensity laser exposure. Such a phase shift may be

associated with a nonlinear contribution or a thermal-induced variation of refractive index of the sample, giving rise to distinct functional forms for the position dependence of the far-field transmittance. For a nonlinear contribution to the refractive index, the position dependence of the far-field normalized transmittance T_N can be described by the Sheik-Bahae (SB) model [31]

$$T_N(\xi) = 1 - \frac{4\Delta\Phi_0\xi}{(\xi^2+9)(\xi^2+1)}. \quad (1)$$

Here $\xi = z/z_c$ defines the sample position with respect to the lens focus ($z = 0$) and $\Delta\Phi_0$ corresponds to the phase shift in the beam wavefront due to the nonlinear contribution in the refractive index, with $\Delta\Phi_0 = -2\pi n_2 I_0 L_{\text{eff}}/\lambda$, I_0 the incident intensity, n_2 the nonlinear refractive index, and L_{eff} the effective sample thickness. In liquid-crystalline samples, n_2 is mainly associated with the reorientation of the orientational order induced by the optical field [32,33], being sensitive to the incident angle ϕ. It is important to highlight that the SB model predicts that the extreme values (peak and valley) of the Z-scan transmittance take place in $z/z_c \approx \pm 0.86$, resulting in a peak-valley separation of $\Delta z_{pv} \approx 1.72 z_c$.

Concerning thermal-induced variations in the liquid-crystal birefringence, the far-field normalized transmittance exhibits a different functional dependence on the sample position. Considering thermal-induced changes in the optical path due to the propagation of a Gaussian laser beam through a low absorbing sample, the position dependence of the far-field transmittance in the Z-scan measurements is properly depicted by the aberrant thermal lens (TL) model [34]

$$T_N(\xi) = \left[1 - \frac{\theta}{2}\tan^{-1}\left(\frac{2\xi}{3+\xi^2}\right)\right]^2, \quad (2)$$

where θ is the thermal-induced phase shift in the beam wavefront associated with the formation of a thermal lens in the sample. More specifically, such a parameter reflects the conversion of the absorbed energy into heat when a Gaussian laser beam passes through the sample, leading to the local heating modification of the liquid-crystal birefringence [26,35], with $\theta \propto d\Delta n/dT$. Here Δn is the birefringence, which depends on the incident angle ϕ and the sample temperature [33]. In the thermal lens model, the extreme values of the far-field transmittance occur at the position $z/z_c = \pm\sqrt{3}$, with $\Delta z_{pv} \approx 3.46 z_c$.

B. Open-aperture configuration

In the configuration of a fully open aperture ($S = 1$), the Z-scan technique is not sensitive to thermally induced changes and nonlinear optical contribution to the refractive index of the sample. In particular, the variation in the far-field transmittance with the sample position is governed by the emergence of a nonlinear contribution to the sample absorption. For a Gaussian laser beam, the SB model defines that the position dependence of the normalized transmittance in the configuration of a fully open aperture can be expressed by

$$T_N(\xi) \approx 1 - \frac{\beta I_0 L_{\text{eff}}}{8^{1/2}[1+\xi^2]}, \quad (3)$$

where β is the nonlinear absorption coefficient, I_0 is the incident intensity, and $L_{\text{eff}} = (1 - e^{-\alpha\ell_0})/\alpha$, with α being the linear absorption coefficient. The saturation of the single-photon absorption is characterized by $\beta < 0$, while $\beta > 0$ corresponds to the multiphoton absorption [31]. By using Eq. (3), it is possible to determine the nonlinear absorption coefficient from the fitting of the normalized transmittance obtained with $S = 1$.

IV. RESULTS

The extinction spectra of the homeotropic 8CB sample containing gold nanorods is exhibited in Fig. 1. The spectra were recorded at distinct temperatures, using an unpolarized light source. In the nematic phase ($T = 309$ K), we observe the typical surface plasmon resonances of gold nanorods presenting an average length $L = 40$ nm, with an aspect ratio around $r = 2.5$ (see the inset). More specifically, the spectrum at $T = 309$ K presents two peaks centered at $\lambda_t = 527$ nm and $\lambda_l = 680$ nm, corresponding, respectively, to the transversal and longitudinal surface plasmon resonances of gold nanorods [36]. Further, it is possible to notice that the longitudinal plasmon band exhibits a higher extinction than the transversal one, indicating that the alignment of gold nanorods deviates from the far-field nematic director. In fact, it has been previously demonstrated that the nematic order induces a long-range orientational order of gold nanorods along the far-field director [37], leading to the suppression of the longitudinal plasmon excitation in planar samples when the light polarization is perpendicular to the nematic director [3,5]. On the other hand, thermal fluctuations tend to randomize the alignment of guest nanoparticles around the director, thus favoring the excitation of the longitudinal plasmons of nanorods dispersed in a homeotropic nematic sample. A different scenario is observed below the nematic–smectic-A transition temperature, where a small blueshift takes place in the spectrum as the temperature is reduced. In particular, we notice a strong suppression in the extinction peak corresponding to the longitudinal surface plasmon resonance, indicating an increase in the average alignment of nanorods along the nematic director. Such behavior may be associated with the emergence of the smectic order, which tends to reduce the orientational fluctuations of gold nanorods around the far-field director. Indeed, the introduction of elongated nanoparticles promotes the formation of dislocations as the layered smectic structure emerges, giving rise to a self-organization process of nanorods in order to reduce the high energy cost associated with the distortions in the smectic order.

In Fig. 2 we present the position dependence of the far-field normalized transmittance through a closed aperture of a homeotropic 8CB sample containing gold nanorods, considering different incidence angles. The sample temperature was fixed at 309 K, well above the smectic-A–nematic transition temperature. In the configuration of normal incidence ($\phi = 0^\circ$), we observe the typical valley and peak signature of a Z-scan measurement in a sample presenting a self-focusing behavior, as shown in Fig. 2(a). In particular, we notice that the peak-valley separation is around $3.4 z_c$, suggesting that the phase shift in the beam wavefront is mainly associated with the formation of a thermal lens in the sample. Such an assumption

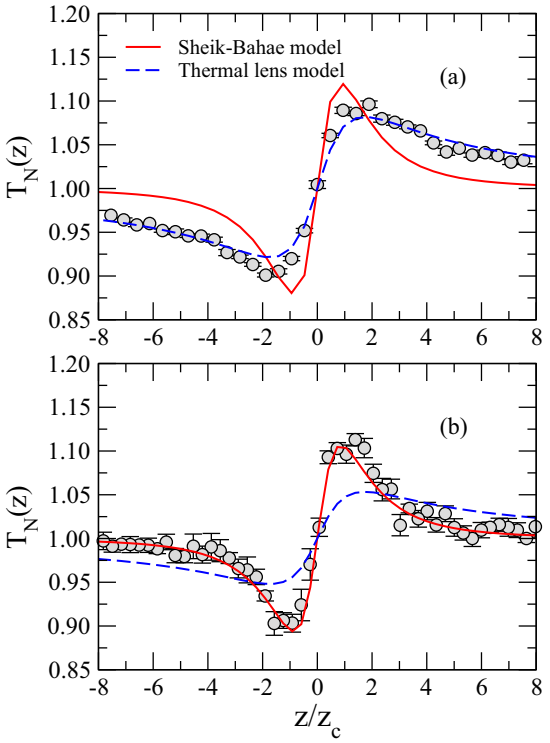

FIG. 2. Normalized Z-scan transmittance of a homeotropic sample of 8CB containing gold nanorods (gray circles), for different incidence angle: (a) $\phi = 0^\circ$ (normal incidence) and (b) $\phi = 5^\circ$ (oblique incidence). The sample temperature was fixed at 309 K, well above the smectic-A–nematic transition temperature. Red solid and blue dashed lines correspond to the best-fit curves using SB and TL models, respectively. Notice that the functional form of the normalized transmittance is strongly sensitive to the incidence angle, indicating that the birefringence changes are governed by different physical mechanisms.

may be verified by using the SB and TL models to fit the experimental data. As one can note, the position dependence of normalized transmittance can be suitably adjusted by the TL model with $\theta = -0.077$ rad. This result indicates that the heat generation from the nonradiative decaying of the plasmon excitation in guest particles induces a thermal variation in the sample birefringence upon the laser exposure in the configuration of normal incidence. A distinct scenario is observed in the configuration of oblique incidence with $\phi = 5^\circ$, as exhibited in Fig. 2(b). Although the self-focusing behavior is preserved, the peak-valley separation is strongly reduced to $1.8z_c$, revealing that the phase shift in the beam wavefront can no longer be assigned to the thermal lens phenomenon. More specifically, an optically induced reorientation of the nematic director takes place in homeotropic samples upon oblique laser incidence, giving rise to a nonlinear optical response [32,33]. Despite the heat generation from plasmon excitation of gold nanorods, such a nematic reorientation induced by the optical field tends to become the main physical mechanism behind the phase shift in the beam wavefront, being characterized by a nonlinear contribution to the sample birefringence. In fact, the dependence of far-field transmittance on the sample position is reasonably fitted by the SB model even for a small incidence angle, with $\Delta\Phi_0 = -0.523$ rad.

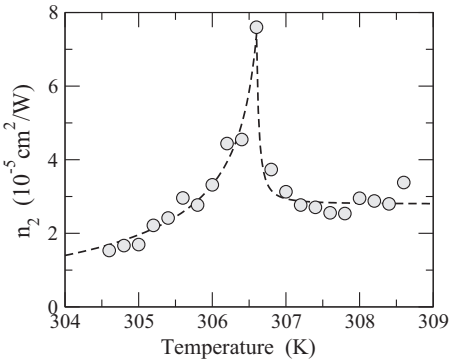

FIG. 3. Temperature dependence of nonlinear refractive index n_2 for a homeotropic 8CB sample containing gold nanorods. The dashed line is shown to guide the eyes. Notice that the nonlinear refractive index exhibits a pronounced increase in the vicinity of the nematic–smectic-A phase transition.

Considering the regime of small reorientation angle for a homeotropic liquid-crystal sample, the nonlinear contribution to the birefringence is expected to depend on the incidence angle ϕ as follows [32,33]:

$$n_2 = \left[\frac{\varepsilon_a^2 \ell_0^2}{24cK_1}\right] \sin^2(2\phi). \tag{4}$$

Here ε_a is the dielectric anisotropy for an optical electric field, K_1 is the splay elastic constant, and c is the speed of light in vacuum. By using $\varepsilon_a = 0.48$, $\phi = 5^\circ$, and $K_1 = 5.40 \times 10^{-7}$ dyn [38], we estimate $n_2 \approx 1.79 \times 10^{-5}$ cm^2/W for the undoped 8CB liquid crystal. In Z-scan measurements performed in pure 8CB samples upon oblique incidence ($\phi = 5^\circ$), a value similar to the nonlinear refractive index is obtained with $n_2 = 1.73 \times 10^{-5}$ cm^2/W. Considering the phase shift for the 8CB sample containing gold nanorods ($\Delta\Phi_0 = -0.523$), we obtain $n_2 \approx 3.48 \times 10^{-5}$ cm^2/W, which is almost twice the estimated value for the undoped sample. Such a result indicates that the addition of gold nanorods amplifies the effects of the optical field on the nematic reorientation. Previous studies reported that the addition of gold nanorods induces a pronounced reduction in the splay elastic constant [14,15,39] and the threshold voltage [39,40] of cyanobiphenyl liquid crystals, while dielectric anisotropy is slightly enhanced [41]. In fact, a reduction in the splay elastic constant leads to an increase of the nonlinear refractive index, as predicted by Eq. (4).

The temperature dependence of the nonlinear contribution to the refractive index is presented in Fig. 3. Here it is possible to observe a pronounced increase of the nonlinear refractive index close to the nematic–smectic-A transition temperature $T_{AN} = 306.5$ K. This result is in contrast with the thermal behavior predicted by Eq. (4). In particular, the dielectric anisotropy tends to exhibit a small increase as $T \to T_{AN}$ [42], while the splay elastic constant remains unchanged [43,44]. However, the anomalous increase of the nonlinear refractive index may be associated with a thermally induced change in the relative angle between the optical field and the nematic director. More specifically, an inhomogeneous reorientation phenomenon may occur due to the emergence of a spatial

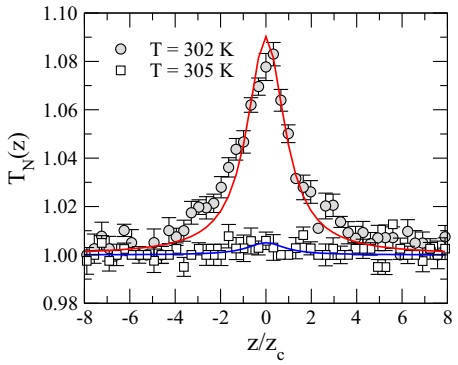

FIG. 4. Normalized Z-scan transmittance of 8CB doped gold nanorods at different temperatures: $T = 302$ K (gray circles) and $T = 305$ K (white squares). The Z-scan measurements were carried out in the configuration of a fully open aperture. The blue and red lines correspond to the best fits using Eq. (3).

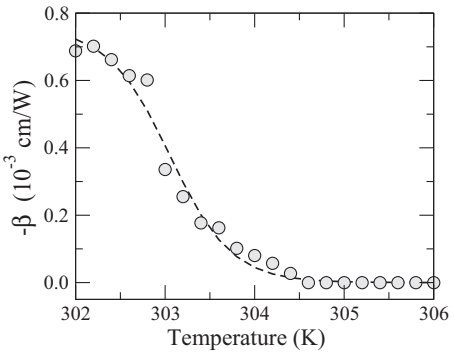

FIG. 5. Temperature dependence of the nonlinear absorption coefficient β of homeotropic 8CB samples doped with gold nanorods. The dashed line is shown to guide the eyes. Notice that the nonlinear absorption coefficient tends to a constant value well below the nematic–smectic-A transition temperature, reflecting the ordering degree of nanorods inside the smectic host as the temperature is reduced.

instability in the orientational order of a homeotropic sample at the vicinity of the nematic–smectic-A phase transition [45–47]. Such a spatial instability corresponds to the distortions in the nematic director resulting from the enhancement of the elastic anisotropy close to nematic–smectic-A phase transition [45], when an external field is applied [46] or orientational fluctuations in the homeotropic anchoring condition take place [47]. As the elastic anisotropy of the nematic phase increases, the spatial instability tends to modify the relative angle between the director and beam propagation direction, thus leading to an enhancement in the nonlinear optical response of the sample as $T \rightarrow T_{AN}$. Below the transition temperature, the spatial instability in the director nematic is suppressed as the smectic order emerges, because the high energy cost associated with the compression of the smectic layers. As a consequence, the nonlinear contribution to the refractive index decreases significantly as the smectic order becomes well established.

Let us now consider the emergence of a nonlinear absorption phenomenon in the smectic phase associated with the addition of gold nanorods. In Fig. 4 we present the far-field normalized transmittance of a homeotropic 8CB sample doped with gold nanorods for Z-scan measurements carried out in the configuration of a fully open aperture ($S = 1$). Again we consider the regime of oblique incidence, with $\phi = 5^\circ$. Close to the transition temperature ($T = 305$ K), we observe that the normalized transmittance stays almost constant as the sample is moved around the focal position $z = 0$. As the temperature is reduced, the normalized transmittance exhibits a maximum at the focal position ($z = 0$), which is typical of a saturation in the single-photon absorption. This nonlinear phenomenon is strongly sensitive to the sample temperature, being pronounced well below the nematic–smectic-A transition temperature. This result suggests that the absorptive nonlinearity is mainly associated with the suppression of the orientational fluctuations of gold nanorods due to the emergence of the smectic order. It is important to stress that this nonlinear optical response can also be observed in the normal incidence geometry [26], indicating that the relative orientation between the nematic director and the optical electric field does not play a significant role in this phenomenon.

In Fig. 5 we present the temperature dependence of $-\beta$ for the homeotropic 8CB sample containing gold nanorods. In particular, the nonlinear absorption coefficient was obtained from the best fits of the Z-scan measurements in the configuration of fully open aperture ($S = 1$), using the SB model defined in Eq. (3). In particular, the incident intensity was varied over the range $I_0 = 5$–20 kW/cm^2. Due to the small linear absorption coefficient at the wavelength of the excitation laser beam ($\alpha < 1$ cm^{-1}), we used $L_{\text{eff}} \approx \ell_0$ for all temperatures. As one can observe, the absolute value of the nonlinear absorption coefficient increases as the sample temperature is reduced, reaching a constant value well below the nematic–smectic-A transition temperature. Such behavior seems to reflect the ordering degree of nanorods as the temperature is reduced. More specifically, the presence of guest particles induces the formation of dislocations in the smectic layered structure, giving rise to a self-organization of nanorods in order to reduce the high energy cost associated with the elastic distortions in the smectic order. As a consequence, the equilibrium configuration may favor the alignment of elongated nanoparticles, thus leading to the saturation of the linear absorption of plasmon bands. Similar behavior has been observed in polymeric films, where an enhanced absorptive nonlinearity is obtained from the nanorods alignment induced by the film stretching [48]. It is important to highlight that the reduction of elastic distortions has been identified in previous studies as the main mechanism behind the formation of linear and curved arrays of spherical nanoparticles in homeotropic 8CB samples in the vicinity of the nematic–smectic-A phase transition [25]. Further, linear defects in the smectic-A phase may trap guest nanoparticles with a rodlike shape, resulting in the formation of linear assemblies aligned along the defect lines [29].

V. CONCLUSION

We have studied the temperature dependence of the nonlinear optical properties in a homeotropic 8CB sample containing gold nanorods. The analysis of the extinction

spectra revealed that the thermal fluctuations in the alignment of gold nanorods are strongly suppressed in the smectic phase, indicating that the smectic ordering may play an important role in self-organization phenomena involving anisotropic guest particles. By using the Z-scan technique in the configuration of a closed aperture, we showed that the changes in the sample birefringence may be governed by distinct physical mechanisms, depending on relative angle between the far-field director and the wave vector of the excitation laser beam. In particular, our result demonstrated that the thermal lens phenomenon is the main mechanism behind the changes in the sample birefringence in the configuration of normal incidence, while the optically induced reorientation of the nematic director becomes the main contribution upon oblique laser excitation. Further, it was verified that the addition of gold nanorods amplifies the optically induced reorientation phenomenon in the homeotropic liquid-crystal sample, presenting a larger nonlinear refractive index than an undoped one. Our results suggest that the addition of gold nanorods may affect the interplay of thermal and reorientation nonlinearities in liquid crystals, with the predominance of each contribution to the self-phase modulation phenomenon being determined by the relative orientation between light polarization and the nematic director. As the self-phase modulation is an important physical mechanism to nonlocal optical phenomena, the control of the interplay of the thermal and reorientation nonlinearities may be of fundamental relevance to the generation and propagation of nonlocal spatial solitons in these samples [49–51]. Close to the nematic–smectic-A phase transition, it was observed that the nonlinear contribution to the liquid-crystal birefringence exhibits an anomalous increasing behavior, which may be associated with the emergence of a spatial instability in the orientational order of a homeotropic sample as its elastic anisotropy increases [45,46]. In Z-scan measurements carried out in the configuration of a fully open aperture, we noticed that a nonlinear absorptive response takes place in 8CB liquid crystal containing gold nanorods only at temperatures where the smectic order is well established. More specifically, it was observed that the absolute value of the nonlinear absorption coefficient increases gradually until reaching a constant value as the sample temperature is reduced. Such behavior seems to be directly related to the enhancement in the orientational ordering of the elongated nanoparticles, which tends to reduce the high energy cost associated with the elastic distortion in the smectic structure [24]. In fact, previous studies reported that the effective alignment of gold nanorods in stretched polymeric film gives rise to a saturable absorption phenomenon [48]. The present results show that the introduction of gold nanorods in smectic samples may be a feasible procedure to obtain assembled nanostructures with tunable nonlinear optical properties.

ACKNOWLEDGMENTS

We are grateful to M. L. Lyra for useful discussions. This work was partially supported by Instituto Nacional de Ciência e Tecnologia de Fluidos Complexos, CAPES, CNPq/MCT, FAPEAL, and FINEP (Brazilian research agencies).

[1] Q. Liu, Y. Cui, D. Gardner, X. Li, S. He, and I. I. Smalyukh, Nano Lett. **10**, 1347 (2010).
[2] S. Khatua, W.-S. Chang, P. Swanglap, J. Olson, and S. Link, Nano Lett. **11**, 3797 (2011).
[3] Q. Liu, Y. Yuan, and I. I. Smalyukh, Nano Lett. **14**, 4071 (2014).
[4] Y. Zhang, Q. Liu, H. Mundoor, Y. Yuan, and I. I. Smalyukh, ACS Nano **9**, 3097 (2015).
[5] L. Jiang, H. Mundoor, Q. Liu, and I. I. Smalyukh, ACS Nano Lett. **10**, 7064 (2016).
[6] Q. Liu, B. Senyuk, J. Tang, T. Lee, J. Qian, S. He, and I. I. Smalyukh, Phys. Rev. Lett. **109**, 088301 (2012).
[7] K. C. Chu, C. Y. Chao, Y. F. Chen, Y. C. Wu, and C. C. Chen, Appl. Phys. Lett. **89**, 103107 (2006).
[8] Q. Liu, J. Tang, Y. Zhang, A. Martinez, S. Wang, S. He, T. J. White, and I. I. Smalyukh, Phys. Rev. E **89**, 052505 (2014).
[9] R. Pratibha, K. Park, I. I. Smalyukh, and W. Park, Opt. Express **17**, 19459 (2009).
[10] G. H. Sheetah, Q. Liu, and I. I. Smalyukh, Opt. Lett. **41**, 4899 (2016).
[11] J. Li, Y. Ma, Y. Gu, I.-C. Khoo, and Q. Gong, Appl. Phys. Lett. **98**, 213101 (2011).
[12] E. Zapp, E. Westphal, H. Gallardo, B. de Souza, and I. C. Vieira, Biosens. Bioelectron. **59**, 127 (2014).
[13] P. Karpinski and A. Miniewicz, Europhys. Lett. **88**, 56003 (2009).
[14] K. K. Vardanyan, E. D. Palazzo, and R. D. Walton, Liq. Cryst. **38**, 709 (2011).
[15] P. L. Madhuri, S. K. Prasad, P. Shinde, and B. L. V. Prasad, J. Phys. D **49**, 425304 (2016).
[16] A. Acreman, M. Kaczmarek, and G. D'Alessandro, Phys. Rev. E **90**, 012504 (2014).
[17] O. Kurochkin, Y. K. Murugesan, T. P. Bennett, G. D'Alessandro, Y. Reznikov, B. J. Tang, G. H. Mehl, and M. Kaczmarek, Phys. Chem. Chem. Phys. **18**, 11503 (2016).
[18] G. B. Hadjichristov, Y. G. Marinov, A. G. Petrov, E. Bruno, L. Marino, and N. Scaramuzza, J. Appl. Phys. **115**, 083107 (2014).
[19] D. Lysenko, E. Ouskova, S. Ksondzyk, V. Reshetnyak, L. Cseh, G. Mehl, and Y. Reznikov, Eur. Phys. J. E **35**, 33 (2012).
[20] E. Ouskova, D. Lysenko, S. Ksondzyk, L. Cseh, G. H. Mehl, V. Reshetnyak, and Y. Reznikov, Mol. Cryst. Liq. Cryst. **545**, 123 (2011).
[21] N. Podoliak, D. Bartczak, O. Buchnev, A. G. Kanaras, and M. Kaczmarek, J. Phys. Chem. C **116**, 12934 (2012).
[22] V. M. Lenart, R. F. Turchiello, G. F. Goya, and S. L. Gómez, Braz. J. Phys. **45**, 213 (2015).
[23] L. D. Sio, T. Placido, R. Comparelli, M. L. Curri, N. Tabiryan, and T. J. Bunning, J. Opt. **18**, 125005 (2016).
[24] R. Pratibha, W. Park, and I. I. Smalyukh, J. Appl. Phys. **107**, 063511 (2010).
[25] J. Milette, S. Relaix, C. Lavigne, V. Toader, S. J. Cowling, I. M. Saez, R. B. Lennox, J. W. Goodby, and L. Reven, Soft Matter **8**, 6593 (2012).
[26] P. B. de Melo, A. M. Nunes, L. Omena, S. M. S. do Nascimento, M. G. A. da Silva, M. R. Meneghetti, and I. N. de Oliveira, Phys. Rev. E **92**, 042504 (2015).

[27] S. Kaur, S. P. Singh, A. M. Biradar, A. Choudhary, and K. Sreenivas, Appl. Phys. Lett. **91**, 023120 (2007).
[28] L. Pelliser, M. Manceau, C. Lethiec, D. Coursault, S. Vezzoli, G. Leménager, L. Coolen, M. DeVittorio, F. Pisanello, L. Carbone *et al.*, Adv. Funct. Mater. **25**, 1719 (2015).
[29] I. Gryn, E. Lacaze, L. Carbone, M. Giocondo, and B. Zappone, Adv. Funct. Mater. **26**, 7122 (2016).
[30] M. G. A. da Silva, A. M. Nunes, S. M. P. Meneghetti, and M. R. Meneghetti, C. R. Chem. **16**, 640 (2013).
[31] M. Sheik-Bahae, A. A. Said, T.-H. Wei, D. J. Hagan, and E. W. V. Stryland, IEEE J. Quantum Electron. **26**, 760 (1990).
[32] F. Simoni and O. Francescangeli, J. Phys.: Condens. Matter **11**, R439 (1999).
[33] I. C. Khoo, Prog. Quantum Electron. **38**, 77 (2014).
[34] C. A. Carter and J. M. Harris, Appl. Opt. **23**, 476 (1984).
[35] L. Omena, P. B. de Melo, M. S. S. Pereira, and I. N. de Oliveira, Phys. Rev. E **89**, 052511 (2014).
[36] S. Link, M. B. Mohamed, and M. A. El-Sayed, J. Phys. Chem. B **103**, 3073 (1999).
[37] B. Senyuk, D. Glugla, and I. I. Smalyukh, Phys. Rev. E **88**, 062507 (2013).
[38] E. P. Raynes, J. D. Bunning, M. J. Bradshaw, and T. E. Faber, J. Phys. **46**, 1513 (1985).
[39] M. Mishra, R. S. Dabrowski, J. K. Vij, A. Mishra, and R. Dhar, Liq. Cryst. **42**, 1580 (2015).
[40] S. Khatua, P. Manna, W.-S. Chang, A. Tcherniak, E. Friedlander, E. R. Zubarev, and S. Link, J. Phys. Chem. C **114**, 7251 (2010).
[41] S. Sridevi, S. K. Prasad, G. G. Nair, V. D'Britto, and B. L. V. Prasad, Appl. Phys. Lett. **97**, 151913 (2010).
[42] S. DasGupta, P. Chattopadhyay, and S. K. Roy, Phys. Rev. E **63**, 041703 (2001).
[43] F. Jähnig and F. Brochard, J. Phys. (Paris) **35**, 301 (1974).
[44] P. Oswald and C. Scalliet, Phys. Rev. E **89**, 032504 (2014).
[45] P. E. Cladis and S. Torza, J. Appl. Phys. **46**, 584 (1975).
[46] C. Chevallard and M. G. Clerc, Phys. Rev. E **65**, 011708 (2001).
[47] V. M. Pergamenshchik, I. Lelidis, and V. A. Uzunova, Phys. Rev. E **77**, 041703 (2008).
[48] J. Li, S. Liu, Y. Liu, F. Zhou, and Z.-Y. Li, Appl. Phys. Lett. **96**, 263103 (2010).
[49] C. Conti, M. Peccianti, and G. Assanto, Phys. Rev. Lett. **92**, 113902 (2004).
[50] M. Peccianti and G. Assanto, Phys. Rep. **516**, 147 (2012).
[51] A. Alberucci, U. A. Laudyn, A. Piccardi, M. Kwasny, B. Klus, M. A. Karpierz, and G. Assanto, Phys. Rev. E **96**, 012703 (2017).